Journal of Clinical and Basic Research
Online ISSN: 2538-3736

Fe_3O_4/HA nanocarriers of Curcumin to evaluate the anti-cancer effect in MCF-7

Mehdi Sheikh Arabi [1*], Seyedeh Zahra Hoseini [2]

1. Medical Cellular and Molecular Research Center, Golestan University of Medical Sciences, Gorgan, Iran
2. Biomaterials Research Group, Nanotechnology and Advanced Materials Department, Materials and Energy Research Center (MERC), Tehran, Iran
* Correspondence: Mehdi Sheikh Arabi, Medical Cellular and Molecular Research Center, Golestan University of Medical Sciences, Gorgan, Iran
Email: msheykharabi@goums.ac.ir

Abstract

Background: Using magnetic nanoparticles has significant attention in various domains, including magnetic storage, medical therapies, and magnetic detection. Curcumin (diferuloylmethane), a polyphenol, is a low molecular weight active ingredient of the perennial herb Curcuma longa (commonly known as turmeric).
Methods: The APTES-coated magnetite nanopowders were prepared as carriers for the anticancer drug "Curcumin" through the modified controlled chemical co-precipitation method. The concentration of Curcumin release in the HA-magnetite nanoparticles in 20 ml phosphate buffer (pH 7.4) within the PBS was determined at unique time intervals using UV-Vis Spectrophotometer as finished within the drug loading measurement. The in vitro cytotoxicity of the nanoparticles became assessed through MTT cellular viability assay after treating the MCF-7 breast adenocarcinoma cells with Curcumin-loaded APTES-covered magnetic NPs in addition to unloaded magnetic NPs in line with the manufacturer's commands.
Results: The APTES and HA-coated and uncoated Fe_3O_4 nanoparticles were characterized by XRD, FE-SEM, FT-IR, Raman, and VSM techniques. The size of the Fe_3O_4 nanoparticles and their distribution were determined by Hydrodynamic length distribution. TEM results revealed that the average particle size is 15 nm. The VSM measurements showed that magnetic particles were superparamagnetic characteristics. Rapid Curcumin drug loading in 2 hrs and the controlled drug release in 1 hr ~15% and 48 hrs ~80% drug release was observed, applying to in-vitro applications. The obtained findings indicated that the APTES- Fe_3O_4/HA nanoparticles are promising for targeted Curcumin drug delivery applications.
Conclusion: Curcumin-loaded MNPs were more potent than free Curcumin for inhibiting MCF-7 cell proliferation due to enhanced uptake in breast cancer cells. Due to high inherent magnetic properties, we may use the nanomedicine platforms for theranostic application after ensuring the MRI imaging abilities.

Article History

Received: 17 August 2022
Received in revised form: 1 September 2022
Accepted: 11 September 2022
Published online: 15 July 2023

DOI: 10.29252/JCBR.7.1.25

Keywords

Fe_3O_4
Curcumin
Hyaluronic acid
Magnetic nanoparticles
MCF-7
Cancer

Article Type: Original Article

Highlights

Nanoscale drug delivery systems constitute an evolving drug delivery and tumor targeting approach.
Multilayer MNPs coated with polymers are great candidates for efficient drug delivery programs.

Introduction

Magnetic nanoparticles have attracted much interest, now not only handiest in magnetic recording but also in the medical therapy and magnetic sensing areas. Specifically, superparamagnetic iron oxide nanoparticles (Fe_3O_4 and γ -Fe_2O_3) with tailored surface chemistry were extensively used for several in vivo biomedical applications, including drug delivery systems (DDS), magnetic resonance imaging (MRI), most cancers therapy, tissue regeneration, immunoassay, detoxing of organic fluids, hyperthermia, drug delivery, and cell separation (1). Alternatively, silica-based drug-delivery carriers are chemically and thermally extra solid, highly hydrophilic, biocompatible, and may be easily functionalized for bio-conjugation purposes. Hence, silica-lined magnetite nanoparticles (Fe_3O_4-SiO_2/core-shell) were synthesized via many groups (2, 3).

Hyaluronic acid is the main component of the extracellular matrix and is widely distributed in vertebrate tissues. The skin contains over 50% of the total hyaluronic acid in the body, and its structural function relies on its distinct hydrodynamic characteristics and how it interacts with other elements of the extracellular matrix (4).

Curcumin (diferuloylmethane), a polyphenol, is a low molecular weight active principle of the perennial herb Curcuma longa (commonly known as turmeric). Curcumin possesses antioxidant (5), anti-inflammatory (6), anti-carcinogenic, and antimicrobial (7) properties and suppresses the proliferation of various tumor cells. Several clinical trials dealing with cancer have addressed Curcumin's pharmacokinetics, safety, and efficacy in humans. Despite extensive research and development, poor solubility of Curcumin in aqueous solution remains a major obstacle to its bioavailability and clinical efficacy (8).

This study involves creating carriers made of Fe_3O_4/HA nanoparticles with superparamagnetic properties and coated with APTES (Figure 1. Chem Draw.16). The organosilane can either adsorb or bond covalently with iron oxide. At the same time, its active amino group can react with the Curcumin cancer medication. A novel aspect of this research involved connecting Curcumin to iron oxide nanoparticles coated with APTES and HA. This study's findings showed that these Curcumin-loaded nanoparticles were more effective in treating MCF-7 cells (Figure 2), indicating their increased uptake and improved healing capabilities. Besides, this study examined these nanoparticles' drug loading and in vitro drug release, demonstrating their potential as magnetic carriers for targeted drug delivery.

Figure 1. Schematic structure of Fe_3O_4/HA nanoparticles with Curcumin loading

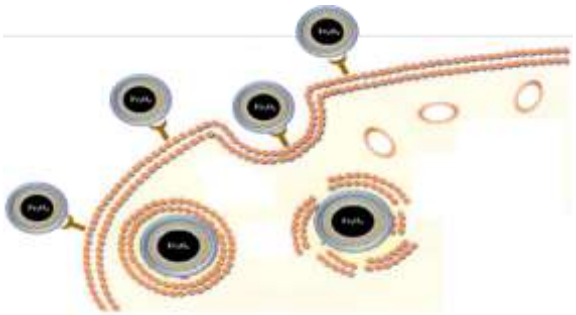

Figure 2. Interaction between Fe_3O_4/HA nanocarrier with MCF-7 cells

Methods

$Fe(NO3)3{\cdot}9H_2O$, $FeSO_4{\cdot}7H_2O$, NaOH, sulfate heptahydrate ($FeSO_4.7H_2O$), ammonium hydroxide ($NH_3.H_2O$), oleic acid, Hyaluronic acid (HA), Tetrahydrofuran (THF), (3-Aminopropyl) triethoxysilane (APTES) and ethanol were purchased from Merck (Germany). $NH_2OH{\cdot}HCl$, trisodium citrate, dithiothreitol (DTT), Tris buffer acetate-EDTA (TAE), LysoTracker-Red, Paclitaxel (PTX), sodium tetrachloroaurate, dimethyl sulfoxide (DMSO) and MTT (3- (4, 5 dimethylthiazol-2-yl)-2, 5-diphenyltetrazolium bromide) and 0.4% formaldehyde solution were bought from Sigma (USA). The Fetal bovine serum (FBS), Trypsin–EDTA (0.25%), and DMEM materials were purchased from Gibco.

Preparation of Fe_3O_4 nanoparticles

Magnetite turned into made in keeping with the modified method of Molday (15). The standard experimental technique prepared 30 ml of 0.1M ferric chloride hexahydrate and 15 ml of 0.1M ferrous sulfate heptahydrate solutions by dissolving respective iron salts in 1M HCl. The mixture of the iron solution changed into stirred, followed by the slow addition of ammonia ($NH_3.H_2O$) to bring the pH=11. All through the addition of $NH_3.H_2O$, the yellow-orange mixture changed from light brown to black. About 5ml of oleic acid became introduced, and the vigorous stirring persisted for 1 hr at 70 °C. The formed magnetite nanoparticles were centrifuged at 10,000 rpm for 15 minutes, then decanted using the outside magnet. The obtained magnetite nanoparticles were then washed using water and ethanol and dried in a vacuum.

Synthesis of Fe_3O_4 nanoparticles coated with APTES

A solution of APTES at 5% concentration was created by dissolving it in deionized water and regulating the pH to 4 using acetic acid. Around 0.1 grams of magnetite nanoparticle powder was added to an APTES solution and continuously stirred for 3 hours to create a coating. The APTES-coated magnetic particles were separated from the solution by settling under the influence of a magnetic field generated by a bar magnet and underwent a thorough water wash before being dried.

Preparation of HA-coated Fe_3O_4-APTES nanoparticles

Dialysis was used to create HA/Fe_3O_4-APTES nanoparticles straightforwardly. In summary, a solution was made by dissolving HA polymers in a mixture of THF and deionized water in equal volumes. Next, Fe_3O_4-APTES was evenly mixed with 1mL THF and slowly dripped into a solution of HA copolymer. The mixture was then subjected to 20 minutes of ultrasonic treatment. Subsequently, the solution was subjected to dialysis (with a molecular weight cut off of 3500 Da) against pure water for 24 hours. Ultimately, the resolution was refined using a syringe filter with a pore size of 1 µm. Ultimately, the nanocarrier known as HA/Fe_3O_4-APTES was acquired.

Curcumin drug loading and release studies

The present research was conducted on the loading and releasing a cancer-fighting compound derived from Curcumin using Fe_3O_4 nanoparticles coated with APTES and HA. To increase the absorption of Curcumin, this research employed a method that involved stirring 10mg of APTES-coated Fe_3O_4 nanoparticles in a solution of 0.1% Curcumin dissolved in ethanol for 3 hours. This process was referred to as Curcumin loading, done to enhance the effectiveness of Curcumin as an anti-cancer drug. The magnetite nanoparticles were separated from the mixture at regular intervals using a permanent magnet. The remaining Curcumin in the liquid was then measured at 428 nm using a UV-Vis Spectrophotometer.

Nanoparticle characterization

The infrared spectra involving the Fourier transform were captured across the spectrum from 500 to 4000 cm-1. X-ray diffraction (XRD) data were collected using Cu (Kα) radiation, with a wavelength of 1, 5406 A°, at room temperature. The scanning rate was 0.02° S-1, and data was collected in the 2θ range from 4° to 120°. The dried powder samples were subjected to thermogravimetric analysis in the presence of argon flow and heated from room temperature up to 900°C at a rate of 10°C per minute. The magnetic properties of the prearranged magnetic NPs were investigated using a Vibrating Sample Magnetometer (VSM) with a top magnetic capacity of 10 kOe at 298 K. The UV-Vis spectra for magnetic nanoparticles were measured in the 220-800 nm range. The size range and electrical charge of the MNPs produced were evaluated using dynamic light scattering methodology to determine their hydrodynamic length distribution and zeta potential. In just four minutes at a temperature of 25°C, the dimensions of the particles were accurately determined. The results have been documented from five trials carried out on every magnetic NP. The zeta potential of magnetic nanoparticles was determined by taking an average of three measurements. The structure of the specimens was analyzed using transmission and scanning electron microscopes (TEM and SEM). The behaviour of Curcumin released from magnetic nanoparticles was examined by introducing 2 mg of Curcumin-loaded magnetic nanoparticles into 3 mL of phosphate buffer saline (PBS) with a pH of 5.5 or 7.4 containing 0.1% w/v Tween-80 and analyzing the absorption intensity at 450 nm with the use of ultraviolet-visible spectrophotometry (9).

Cell cytotoxicity

The in vitro cytotoxicity of the nanoparticles became assessed through MTT cellular viability assay after treating the MCF-7 breast adenocarcinoma cells with Curcumin-loaded APTES-covered magnetic NPs in addition to unloaded magnetic NPs in line with the manufacturer's commands. In brief, the cancer cells were seeded right into a 96-well plate at an initial density of 2×103 cells in line with properly in a very last quantity of 100 L DMEM medium accompanied utilizing incubation overnight to convey the cells to confluence. After that, the medium changed into replaced with a 100 L sparkling medium containing natural PBS buffer, Curcumin, and NPs at unique concentrations (5, 10, 20, 40, and 80 M). After incubation time (48 h) at 37°C and 5% CO_2, 10 L of the MTT labelling reagent (final concentration 0.5 mg/mL) become brought to each nicely and incubated for 4 h to locate the metabolically lively cells. Then 100 L DMSO changed into delivered to every nicely to update the culture medium and dissolve the insoluble formazan crystals. After overnight incubation in a humidified environment and 37 °C, the absorbance of each was properly measured using an assay high-tech Eliza reader spectrophotometer at 570 nm. The antiproliferation potential of magnetic NPs treatment becomes calculated as a percentage of cell growth concerning the PBS controls the use of the subsequent equation:

$$\text{viability (\%)} = \frac{\text{A (in 570 nm of treated cells)}}{\text{A (in 570 nm of control cells)}} \times 100$$ Standard deviations were obtained from 3 replicates

Results

Size assessment with SEM and TEM

The appropriate dimensions of particle distributions for the synthesized magnetite particles and the APTES- and HA-coated magnetite NPs were determined using a particle size analyzer with an aquatic solution, and the results can be found in Figure 3. The size of the Fe_3O_4 nanoparticles without coating ranged from 10-22 nm, mostly between 13-17 nm, as depicted in Figure 3. Conversely, the APTES-and HA-coatedFe_3O_4 nanoparticles ranged in size from 20-80 nm.

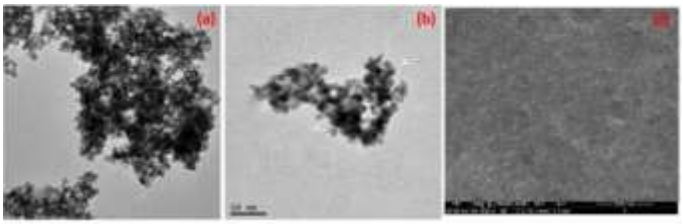

Figure 3. TEM images of APTES/HA coated Fe3O4 nanoparticles and SEM images of Fe_3O_4 nanoparticles

X-ray diffraction

Figures 4a and 4b show the XRD styles of uncoated, APTES, and HA-covered magnetic NPs. The position and relative depth of all diffraction peaks fit nicely with the sample for Fe_3O_4 (JCPDS No. 89-0951), indicating that the samples have a cubic crystal system. No feature peaks for the impurities of Fe-OOH; α-Fe_2O_3 detected. The implied particle crystallite length of the synthesized Fe_3O_4 nanoparticles becomes calculated from the XRD pattern in line with the road width of the (311) plane refraction using Scherrer equation (10).

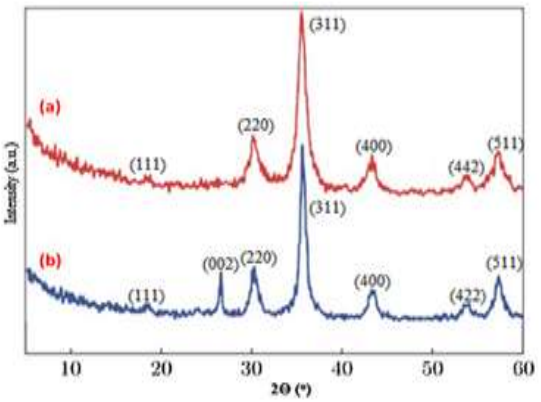

Figure 4. XRD pattern of the a) naked Fe_3O_4 MNPs and b) APTES/HA coated MNP

FT-IR spectrometer

The resulting spectra are offered in Figure 5. The presence of two strong absorption bands at around 585 and 632 cm-1 within Figure 5a, in reality, suggests the formation of magnetic NPs. These bands are fashioned from the cut-up of the vibrational band at 575 cm-1 corresponds to the Fe–O bond of bulk magnetic (11). In Figure 5a, the peak at 3415 cm-1 is attributed to the stretching vibrations of –OH adsorbed on the surface of the Fe_3O_4 nanoparticle. The silica community is adsorbed at the magnetic surface via Fe–O–Si bonds. This adsorption band cannot be seen inside the FT-IR spectrum (Figure 5b) because it usually seems at around 585 cm-1 and consequently overlaps with the Fe–O vibration of magnetic NPs (12, 13).

Within the case of APTES-coated NPs (Figure 5b), the coating of APTES is established via the presence of peaks at ~2925 and ~2815 cm-1 are attributed to the stretching vibrations of -CH_2 and -CH_3 present inside the APTES. The peak at ~1630 cm-1 is assigned bending vibration of N-H present within the APTES. In each of the spectra of uncoated iron oxide NPs and APTES-coated iron oxide NPs, the absence of the C=O stretch at 1700 cm-1 suggests the binding of the carboxylic institution of oleic acid to the iron oxide NPs. Those outcomes confirm that the APTES is covered chemically directly to the surface of the Fe_3O_4 nanoparticles.

In Figure 5c, the presence of Curcumin is found through the arrival of the peak at ~ 2925 cm-1 attributed to the stretching vibration of –C-O-CH_3 group, the aromatic ring C-C stretching vibration is regarded at ~1520 cm^{-1} and the band at 1626 cm-1 indicates the presence of fragrant C-H bending vibration. The reduction of the OH peak indicates the binding of Curcumin to the nanoparticle's surface, reduced the tingle by overlapping the OH peaks in the composition of the magnetic nanoparticle containing Curcumin in the 3400 cm^{-1} region.

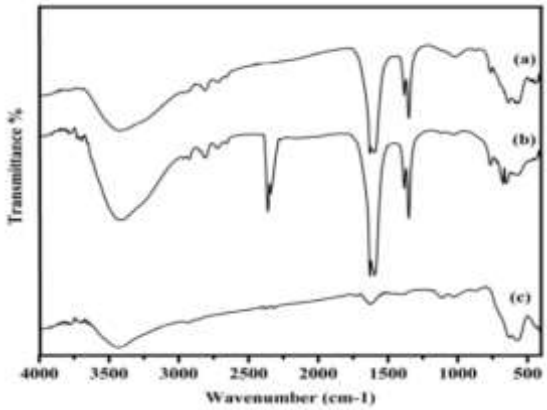

Figure 5. FT-IR Spectra of a) Fe_3O_4 and b) APTES coated Fe_3O_4 c) Curcumin bound APTES coated Fe_3O_4 Nanoparticles

Zeta potential and dynamic light scattering

The particle size information of the magnetic NPs with the aid of DLS becomes near TEM and SEM micrographs (Table 1).

Table 1. The particle size data and Zeta potential data of the MNPs

Nanocarrier	Zeta potential	Hydrodynamic diameter	Polydispersity index
Fe_3O_4	-5	20	1,00
APTES/HA coated Fe_3O_4	-18	40	0,234

TGA

The TG curves in Figure 6, indicate that under an air environment, both Fe_3O_4 NPs and Fe_3O_4 NPs coated with APTES and HA experience a weight reduction below the temperature of 800 °C. The weight loss observed before reaching a temperature of 220°C can be attributed to the expulsion of water or OH molecules absorbed onto the iron oxide surface. The significant decrease in weight during the second phase can be traced back to the deterioration of oleic acid in all variants of Fe_3O_4 NPs, whether they are coated with APTES and HA or not (15).

VSM

According to Figure 7, the hysteresis loops of magnetic nanoparticles exhibit zero coercivity and remanence, indicating that all magnetic nanoparticles exhibit superparamagnetic behavior. The Saturation magnetization of uncoated Fe_3O_4 magnetic NP turned into 90 emu g-1 even as that for APTES and HA lined magnetic NPs have been 69.2 emu g-1, respectively.

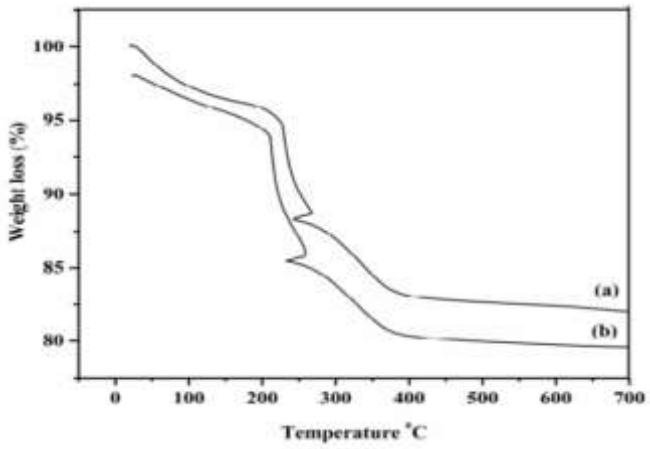

Figure 6. TGA curve for a) Fe_3O_4 and b) APTES/HA coated Fe_3O_4 nanoparticles

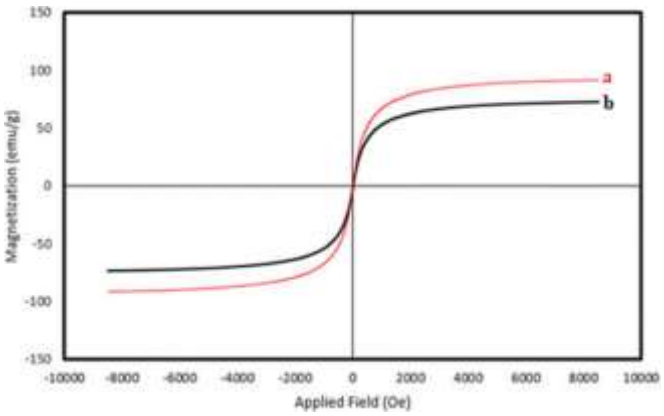

Figure 7a) The maximum magnetization level of Fe_3O_4, and b) The highest magnetization level of Fe_3O_4 nanoparticles coated with APTES/HA

In vitro drug release assay

The loading and releasing performance of APTES and HA-coated Fe_3O_4 nanoparticles is depicted in Figures 8a and 8b. Through analysis of the loading profile (as depicted in Figure 8a), it has been determined that Curcumin has a rapid absorption rate during the early stage, followed by a decline in absorption rate after 60 minutes. This decrease in rate can be attributed to the saturation of the nanoparticles' surface with Curcumin, with the saturation point reaching the 120-minute mark. After 120 minutes of adsorption, no further changes occurred in the Curcumin concentration because the particles had already reached their maximum capacity and could not take in anymore. Based on the discoveries as mentioned earlier, it can be concluded that the highest drug absorption occurs within the short timeframe of 2 hours.

The Curcumin-loaded APTES-Fe_3O_4 and HA NPs were evaluated for their ability to slowly release the substance through testing the leaching of Curcumin in phosphate buffer at the pH of the human body (pH 7. 4), as illustrated in Figures 8b. As time goes on, a noticeable rise was observed in absorbance seen in the UV spectra of the HA NPs and APTES-Fe_3O_4, both of which are loaded with Curcumin and dissolved in buffer solution (18). However, the sustainability of the release rate decreased significantly when the time was extended.

Cell cytotoxicity

Cell viability assay in response to magnetic NPs was used to evaluate the cytotoxicity of the NPs (Figure 9). No full-size impact of the manipulated treatments was located on cell growth. IC50 values (concentrations of 50% MCF-7 most cancers cells increase inhibition) as a quantitative measure for the cytotoxicity had been 40 µM for free Curcumin and 22 and 13 µM for magnetic NP-Curcumin, respectively. This information showed that Curcumin-loaded magnetic NPs had been more powerful than loose Curcumin in suppressing cell proliferation. After treating the MCF-7 cells with unfastened magnetic NPs, all goal carriers were nearly reliable in the given concentration range, as proven in Figures 9 A and B. The lower zeta potential of the NPs can affirm surface rate alteration (Table 1).

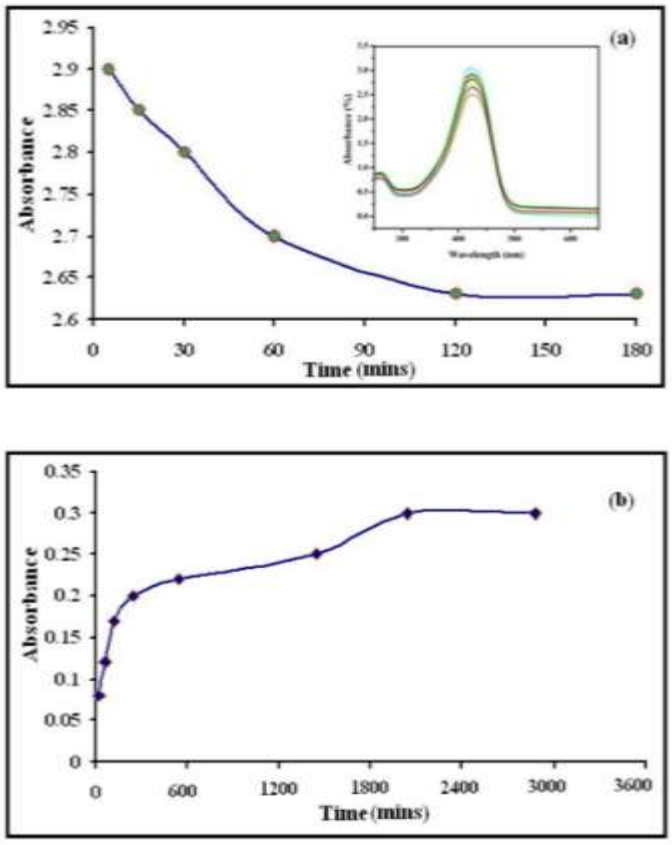

Figure 8a. Curcumin loading on APTES/HA coated Fe3O4 nanoparticles, b. Curcumin release from APTES-coated Fe3O4 nanoparticles in buffer (pH 7.4)

Discussion

We developed nanocarriers with high loading capacity for curcumin, sustained release profile, homocompatibility, biocompatibility and suitable protein pattern. The size range of the formed nanoparticles was very favorable even in the coated condition. The crystallite length of the uncoated Fe_3O_4 nanoparticles received using this method became approximately 12 nm, and for the APTES and HA lined turned to about 15 nm. The moderate distinction among them can be attributed to the water-swollen debris for the DLS dimension compared to the dried state for TEM, and SEM dimensions. The difference in measured sizes between DLS and TEM and SEM has also been mentioned with different nanomaterials (14). The Fe_3O_4 NPs without coating experienced a gradual weight reduction of 6%, whereas the APTES and HA-coated magnetic NPs only exhibited a weight reduction of 3%, according to the TG analysis results. This fact confirms that the APTES molecule has a covalent bond with the -OH found on the surface of the magnetic NPs.

The lower cost of magnetization could be due to the increased mass of the particles on the surface of magnetic nanoparticles when unmagnetized shells are utilized. This saturated magnetization for modified magnetic NPs is enough for magnetic separation or course (16, 17).

According to the release profile, the Curcumin medication displays a rapid onset for the initial 9 hours, followed by a decline in drug release. Two factors may account for these actions: 1) The greater diffusion of drug molecules from the magnetic NPs matrix into the buffer solution, leading to a faster drug release (19), and 2) The gradual release of the drug due to the highly soluble phenolic acidic group present in the ionizable drug, as well as the diminished concentration on the APTES surface (20). Proposedly, magnetic NP-Curcumin broken mitochondrial membrane extra effective than unfastened Curcumin and thus multiplied anticancer potential due to improved uptake of Curcumin (21). Advisingly, Bcl-xL expression is strongly suppressed after remedy with Curcumin-loaded magnetic NP compared to equal amounts of Curcumin (22).

Conclusion

A strong focus on developing formulations exists that possess safe and biocompatible properties while also exhibiting exceptional anticancer properties for biomedical purposes such as drug delivery. The present study constructed nanocarriers that can hold a large amount of Curcumin, release it gradually, are safe for blood circulation, well-suited for biological use, and have a desirable protein corona formation. Additionally, the IC50 measurements indicating the degree of cytotoxicity were 40 µM for Curcumin in its unfettered form. In comparison, the measurements for magnetic NP-Curcumin reached just 13 µM, and for normal NP-Curcumin, 22 µM. This information revealed that Curcumin-loaded magnetic NPs had been more powerful than free Curcumin in suppressing cell proliferation and inhibiting MCF-7 cell proliferation due to improved uptake in breast cancers cells. Because of high inherent magnetic residences, we may also use the nanomedicine structures for a theranostic utility after ensuring the MRI imaging talents. These findings suggest that the evolved multilayer magnetic NPs, covered with polymers and modified, are super applicants for drug transport applications.

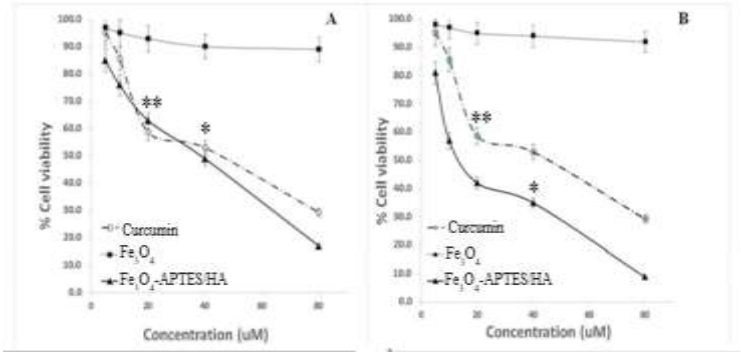

Figure 9. Anti-proliferative effect of free Curcumin and Magnetic nanoparticles. Cell viability of breast cancer cells (MCF-7) was measured using MTT assay by UV-vis spectrophotometer at 492 nm, A) 24 h, and B) 48 h. (When P-value < 0.05, significance was acknowledged. P <0.1 * P <0.01 * P <0.001 **)

Acknowledgements

The financial support for this study was provided by Golestan University of Medical Sciences, Gorgan, Iran.

Funding source

Golestan University of Medical Sciences, Gorgan, Iran, provided financial support for this study under the approval code: 960226237.

Ethical statement

This study was approved by the Ethics Committee of Golestan University of Medical Sciences with an approval code of (IR.GOUMS. REC.1396-265).

Conflict of interest

The authors declared no conflict of interest.

Author contributions

Seyedah Zahra Hosseini performed the laboratory experiments and data analysis and also drafted the manuscript. Mehdi Sheikh Arabi helped in the laboratory experiment and data analysis and in writing the final manuscript.

References

1. Iida H, Takayanagi K, Nakanishi T, Osaka T. Synthesis of Fe3O4 nanoparticles with various sizes and magnetic properties by controlled hydrolysis. J Colloid Interface Sci. 2007;314(1):274-80. [View at Publisher] [Google Scholar] [DOI] [PMID]
2. Tago T, Hatsuta T, Miyajima K, Kishida M, Tashiro S, Wakabayashi K. Novel Synthesis of Silica-Coated Ferrite Nanoparticles Prepared Using Water-in-Oil Microemulsion. Journal of the American Ceramic Society. 2002;85(9):2188-94. [View at Publisher] [Google Scholar] [DOI]
3. Morel AL, Nikitenko SI, Gionnet K, Wattiaux A, Lai-Kee-Him J, Labrugere C, et al. Sonochemical approach to the synthesis of Fe3O4 @SiO2 core - Shell nanoparticles with tunable properties. ACS Nano. 2008;2(5):847-56. [View at Publisher] [Google Scholar] [DOI] [PMID]
4. Dosio F, Arpicco S, Stella B, Fattal E. Hyaluronic acid for anticancer drug and nucleic acid delivery. Adv Drug Deliv Rev. 2016;97:204-36. [View at Publisher] [Google Scholar] [DOI] [PMID]
5. Sreejayan, Rao MNA. Nitric Oxide Scavenging by Curcuminoids. J Pharm Pharmacol. 1997;49(1):105-7. [View at Publisher] [Google Scholar] [DOI] [PMID]
6. Brouet I, Ohshima H. Curcumin, an Anti-tumor Promoter and Anti-inflammatory Agent, Inhibits Induction of Nitric Oxide Synthase in Activated Macrophages. Biochem Biophys Res Commun. 1995;206(2):533-40. doi:10.1006/BBRC.1995.1076 [View at Publisher] [Google Scholar] [DOI] [PMID]

7. Kiso Y, Suzuki Y, Watanabe N, Oshima Y, Hikino H. Antihepatotoxic principles of Curcuma longa rhizomes. Planta Med. 1983;49(3):185-7. [View at Publisher] [Google Scholar] [DOI] [PMID]
8. Tønnesen HH, Karlsen J. Studies on curcumin and curcuminoids. Z Lebensm Unters Forsch. 1985;180(5):402-4. [View at Publisher] [Google Scholar] [DOI] [PMID]
9. Saikia C, Das MK, Ramteke A, Maji TK. Effect of crosslinker on drug delivery properties of curcumin loaded starch coated iron oxide nanoparticles. International journal of biological macromolecules. 2016 Dec 1;93:1121-32. [View at Publisher] [Google Scholar] [DOI] [PMID]
10. Trang VT, Dinh NX, Lan H, et al. APTES Functionalized Iron Oxide–Silver Magnetic Hetero-Nanocomposites for Selective Capture and Rapid Removal of Salmonella enteritidis from Aqueous Solution. Journal of Electronic Materials 2018 47:5. 2018;47(5):2851-60. [View at Publisher] [Google Scholar] [DOI]
11. Waldron RD. Infrared Spectra of Ferrites. Physical Review. 1955;99(6):1727. doi:10.1103/PhysRev.99.1727 [View at Publisher] [Google Scholar] [DOI]
12. Bruni S, Cariati F, Casu M, Lai A, Musinu A, Piccaluga G, et al. IR and NMR study of nanoparticle-support interactions in a Fe2O3-SiO2 nanocomposite prepared by a Sol-gel method. Nanostructured Materials. 1999;11(5):573-86. [View at Publisher] [Google Scholar] [DOI]
13. Guang-She L, Li-Ping L, Smith RL, Inomata H. Characterization of the dispersion process for NiFe2O4 nanocrystals in a silica matrix with infrared spectroscopy and electron paramagnetic resonance. J Mol Struct. 2001;560(1-3):87-93. [View at Publisher] [Google Scholar] [DOI]
14. Akrami M, Khoobi M, Khalilvand-Sedagheh M, et al. Evaluation of multilayer coated magnetic nanoparticles as biocompatible curcumin delivery platforms for breast cancer treatment. RSC Adv. 2015;5(107):88096-107. [View at Publisher] [Google Scholar] [DOI]
15. Jiang W, Wu Y, He B, Zeng X, Lai K, Gu Z. Effect of sodium oleate as a buffer on the synthesis of superparamagnetic magnetite colloids. J Colloid Interface Sci. 2010;347(1):1-7. [View at Publisher] [Google Scholar] [DOI] [PMID]
16. Chaleawlert-Umpon S, Pimpha N. Morphology-controlled magnetite nanoclusters via polyethyleneimine-mediated solvothermal process. Mater Chem Phys. 2012;135(1):1-5. [View at Publisher] [Google Scholar] [DOI]
17. Kuo CH, Liu YC, Chang CMJ, Chen JH, Chang C, Shieh CJ. Optimum conditions for lipase immobilization on chitosan-coated Fe3O4 nanoparticles. Carbohydr Polym. 2012;87(4):2538-45. [View at Publisher] [Google Scholar] [DOI]
18. Chin SF, Iyer KS, Saunders M, St. Pierre TG, Buckley C, Paskevicius M, Raston CL. Encapsulation and sustained release of curcumin using superparamagnetic silica reservoirs. Chemistry–A European Journal. 2009 Jun 2;15(23):5661-5. [View at Publisher] [Google Scholar] [DOI] [PMID].
19. Zhu L, Ma J, Jia N, Zhao Y, Shen H. Chitosan-coated magnetic nanoparticles as carriers of 5-Fluorouracil: Preparation, characterization and cytotoxicity studies. Colloids Surf B Biointerfaces. 2009;68(1):1-6. [View at Publisher] [Google Scholar] [DOI] [PMID]
20. Völgyi G, Baka E, Box KJ, Comer JEA, Takács-Novák K. Study of pH-dependent solubility of organic bases. Revisit of Henderson-Hasselbalch relationship. Anal Chim Acta. 2010;673(1):40-6. [View at Publisher] [Google Scholar] [DOI] [PMID]
21. Yallapu MM, Othman SF, Curtis ET, Bauer NA, Chauhan N, Kumar D, et al. Curcumin-loaded magnetic nanoparticles for breast cancer therapeutics and imaging applications. Int J Nanomedicine. 2012;7:1761-79. [View at Publisher] [Google Scholar] [DOI] [PMID]
22. Banerjee SS, Chen DH. Magnetic Nanoparticles Grafted with Cyclodextrin for Hydrophobic Drug Delivery. Chemistry of Materials. 2007;19(25):6345-9.[View at Publisher] [Google Scholar] [DOI]

How to Cite:

Sheikh Arabi M, Hoseini S.Z. Fe_3O_4/HA nanocarriers of Curcumin to evaluate the anti-cancer effect in MCF-7. *JCBR*. 2023;7(1):25-9.